VOLUME - 11, ISSUE - 05, MAY - 2022 • PRINT ISSN No. 2277 - 8160 • DOI : 10.36106/gjra

Original Research Paper

Medical Physics

SPECTROSCOPY AND DOSIMETRY OF SECONDARY RADIATION FOR RADIOLOGY SYSTEMS

Ioannis S. Vlachos Doctorate Thesis.

KEYWORDS :

CHAPTER A: *THEORETICAL PART*

INTRODUCTION

The Problem

We now know that the primary sources of radiation dose for humans is the natural radiation and medical applications of radiation. The contribution from all the medical uses in annual per capita dose varies from a few centimeters dose from the natural environment in developing countries by significantly higher rates in developed countries. The bulk of this contribution comes, according to studies from diagnostic radiology. It is therefore appropriate to review the radio diagnostic examinations, which are not important information in the diagnosis are expected to contribute, while minimizing the doses of beneficial radiological examinations.

The radiation in medical imaging acquired particular interest since the beginning of last century. The machines and methods have evolved since then in order to protect the patient from the existent damaging effects of -rays [Vanbeckevoort *et al* 1995, Archer *et al* 2005]. The degree of security in modern diagnostic radiology, it is now high and a radiological examination when recommended based on the clinical judgment of a qualified medical practitioner is expected to bring the patient benefits that outweigh the potential risk. However, there is no justification in the case that a radiographic examinations unacceptable doses. Always apply the principles of ALARA so that all doses be kept as low as reasonably achievable, without losing the necessary diagnostic and clinical information. Therefore, in carrying out the relevant radiological examinations should be given by staff due attention to maintain the absorbed dose to staff and patients at lower levels compared to the corresponding Diagnostic Levels Reference (CMP), without reducing the diagnostic value examination.

Dose from diagnostic X-ray equipment is delivered from the primary X-rays, the scattered X-rays, and the leakage of the X-ray tube. To calculate the effective dose it is necessary to determine all three [Noto *et al* 2003, Noto *et al* 2009]. An important part of determining the radiation protection requirements during X-ray room design is the calculation of the amount of scatter inside and outside the planned locations of the shielding barriers [Mc Vey *et al* 2004, Petrantonaki et al 1999].

Radiation protection and dosimetry in medical X-ray imaging practice has been extensively studied during the last decades. In the last decades, there has been an extended scientific discussion concerning radiation protection and dosimetry in 3medical X-ray imaging practice [McCullough *et al* 1970, International Atomic Energy Agency (IAEA) 2004, IAEA Safety Reports 2006].

The presence of different equipment and X-ray practices not only affects the dose of the patients, but the dose of the personnel, as well. The variety of the available equipment and X-ray practices not only affect the dose the patient receives, but also affects the dose received by the personnel [Simpkin *et al* 1998].

A significant number of studies and efforts today towards limiting the dose to the patient per test and to protect workers. Manufacturing companies of both machines, and the radio protective materials have the common aim of reducing the dose. Within this new modern efforts Radiography Systems placed on the market and new shielding materials are then tested for effective protection of personnel from scattered radiation, particularly in interventional radiology [Archer *et al* 2005]. The limelight have seen studies related both to materials and methods of shielding Radiology Halls, and the materials and methods of special protective equipment used by workers [Clarke *et al* 2005, Jackson *et al* 2006, International Commission on Radiological Protection 2007, Wrixon *et al* 2008, Ohba *et al* 2009].

Thesis Originality

The scope of this thesis was to study the secondary radiation in radiographic rooms. This is useful for in bed radiographs or cases when the examinee is supported by accompanied persons. In addition we have studied the effect of common building materials as radiation shields for dental and veterinary applications. The measurements were performed in the Department of the Sismanoglio General Hospital of Athens, Greece. This was achieved by special measuring equipment, with a conventional radiation modality and with some common building materials.

- An Amptek XR-100 CdTe spectrometer was used for measuring secondary X-rays and energy distribution. The response of the spectrometer for various energies in terms of energy per bin and detector quantum efficiency per energy value were known through calibration in various radiation energies and published literature [Abbene *et al* 2007, Martini *et al* 2015, Vlachos *et al* 2015].

- Common building materials: a) single ceramic tile, b) reinforced ceramic tile, c) double reinforced ceramic tile, d) glass block, e) single plasterboard (or gypsumboard wall) and f) double plasterboard [Vlachos *et al* 2015].

Results showed that the secondary radiation and the energy spectrum are different, using different irradiation fields and keeping stable the tube voltage at 70 kVp in dental and veterinary radiology. It has been shown the secondary radiation and the dose rate (mSv/hr) was reduced at 16 cm x 2 cm irradiation field (for Panoramic radiograph) with respect to the 7.5 cm x 7.5 cm irradiation field (for Cone beam computed tomography). In addition the average transmitted X-ray energy and the dose area was reduce in 16 cm x 2 cm irradiation field compared to 7.5 cm x 7.5 cm irradiation field. In the present work the method was evaluated by measuring equipment and the X-ray generator and X-ray tube [Vlachos *et al* 2015].

Moreover this study are of value during exposure of people not protected by shielding materials such as radiographers, and patients during the use of mobile X-ray units, since it has demonstrated that the choice of the tube voltage and filtration affects the dose rate from the scatter radiation [Vlachos *et al* 2015].

Finally this thesis answered the problem regarding the radiological protection from common building materials for

low energy X-rays meanly in dental and veterinary radiology, using the appropriate metric equipment. The radio protection in dental and veterinary radiology, testing common building materials such as, ceramic tiles, glass block and plasterboard, of the photon energy spectrum and the secondary diagnostic X-rays [Vlachos *et al* 2015].

Publications

Publications In Peer Reviewed International Journals With Impact Factor.

- I. Vlachos, X. Tsantilas, N. Kalyvas, H. Delis, I. Kandarakis, G. Panayiotakis. *Measuring scatter radiation in diagnostic X rays for radiation protection purposes*. Radiation Protection Dosimetry (2015) **165** 382-385, doi:10.1093/rpd/ncv093.

Publications In Peer Reviewed International Proceedings.

- I. Vlachos, X. Tsantilas, G. Fountos, H. Delis, I. Kandarakis, G. Panayiotakis. *Effect of common building materials in narrow shaped X-ray fields transmission*. Journal of Physics: Conference Series **637** (2015) 012034, doi:10.1088/1742-6596/637/1/012034.

Publications Or Abstracts In International Conference Proceedings.

- I. Vlachos, N. Kalyvas, X. Tsantilas, G. Fountos, H. Delis, I. Kandarakis, G. Panayiotakis. *Secondary radiation transmission from common building materials for radiation protection in dental and veterinary radiographic applications*. International Conference "Science in Technology" (SCinTE 2015) , November 5-7, 2015, Technological Educational Institute (TEI) of Athens, Greece.
- I. Vlachos, X. Tsantilas, G. Fountos, H Delis, I. Kandarakis, G. Panayiotakis. *Effect of common building materials in narrow shaped X-ray fields transmission*. International Conference on Bio-Medical Instrumentation and related Engineering and Physical Sciences (BIOMEP 2015), June 18-20, 2015, Technological Educational Institute (TEI) of Athens, Greece.
- I. Vlachos, X. Tsantilas, N. Kalyvas, H. Delis, I. Kandarakis, G. Panayiotakis. *Measuring scatter radiation in diagnostic X rays for radiation protection*. International Conference on Radiation Protection in Medicine (RPM 2014), 30 May - 2 June 2014, Varna, Bulgaria.
- N. Kalyvas, I. Vlachos, X. Tsantilas, I. Kandarakis, G. Panayiotakis. *Measurement of scatter radiation spectrum from radiographic units*. European Society of Radiology (ECR 2013), March 7-11, 2013, Vienna, Austria.

A.2 Radiation Quantities And Units

Radiation Quantities And Units

Absorbed dose D - The definition of absorbed dose given from ICRU 1960 is: D = dE/dm, where dE is the mean energy imparted by the ionising radiation to a material of mass dm. The SI units of absorbed dose are Jkg^{-1} which has been given the special name gray (Gy). Absorbed dose is incomplete without a reference to the material concerned (absorbed dose in water). It is measured in Gy, 1 Gy = 1 joules/kilogram. The old unit of adsorbed dose was the rad, 1 Gy = 100 rads [Greening 1985, U.S Food and Drag Admistration 2015].

Dose Equivalent - The most common simplification is to assess the maximum absorber dose or dose equivalent occurring in the body. Under most circumstances the maximum dose equivalent occurs at very nearly the same depth in the body as the maximum absorbed dose. Sievert (Sv) is the unit for the quantity equivalent dose, where equivalent dose (in Sv) = absorbed dose (in Gy) x radiation weighting factor [Greening 1985, U.S Food and Drag Admistration 2015].

Effective dose equivalent - ICRP set the limits for dose equivalent for dose equivalent are based on an assumption of uniform irradiation of the body. In practice this is very rare. Different tissues have different susceptibilities to radiation. ICRP defined effective dose equivalent, $H_E = \Sigma_{WT} \cdot H_T$, where $_{WT}$ is a weighting factor arising from uniform irradiation of the whole body and H_T the dose equivalent in tissue [Greening 1985].

Exposure X - Ionising radiation have often been measured by the ionisation they produce. Early investigation of X-rays and electrons were made by observing the ionisation produced in gases. The unit for exposure is the roentgen ®, and the SI unit is the coulomb per kilogram of air (C/kg):
$1 R = 2.58 \times 10^{-4} C/kg$ (1)

The exposure can be readily measured through an ionization chamber [Sprawls *et al* 1995].

KERMA-

Kinetic Energy Released per unit MAss (of air). This quantity was introduced to emphasise the two stage process that occurs when indirectly ionising 8radiation deposits energy in matter. KERMA, is expressed in J/kg which is also the radiation unit, the gray (G) [Greening 1985, Sprawls *et al* 1995].

A.3 X-RAYS

X-ray Tubes / Generators

The cathode is the source of electrons and the anode which acts as an electron target. The cathode and the anode are contained in a glass envelope, which provides vacuum, support and electrical insulation and all this system is powered by the generator. The distribution of energy and the quantity of the photons are controlled by adjusting the voltage (kV) or the potential applied to the tube and current (mA) that flows through the tube and exposure time (sec) [Radiopaedia 2015].

The X-rays produced by accelerating electrons with a high voltage and allowing them to collide with the focal spot of anode. These X-rays are called Brehmsstrahlung. Another part of the X-ray spectrum demonstrated high peaks called "Characteristic X-rays", due to the interactions of K-shell electron. The electron in the K-shell may be ejected and leave a 'hole', which is filled by an outer shell electron with an emission of a single X-ray photon [Radiopaedia 2015].

A.4 Photon Interactions

Photoelectric

The interaction is with the atom as a whole, and it cannot take place with free electrons. The collision of a photon whose energy is greater than the binding energy of a tightly bound orbital electron with that electron. The photon disappears and the electron is ejected from the shell. A vacancy is left in the atom, the entire E = hv is transferred to the electron. The product of the interaction is a photoelectron, whose kinetic energy is KE = hv-EB (EB is the binding energy). The photoelectron dissipates its energy in the medium by excitation and ionization. The binding energy is transferred to the absorber by means of fluorescent radiation that follows the initial interaction [Greening 1985].

Compton

The interaction takes place between the photon and a 'free' electron of the medium energy to the electron (assumed initially in rest), known as recoil electron. In a collision between a photon and a free electron it is impossible for all the photon's energy to be transferred to the electron, as it should be v = c. All angles of scattering are possible, so the energy transferred vary from zero to the photon's energy [Greening 1985].

Coherent Scatter

An E/M wave passes near the electron and sets it into oscillation. The oscillating e^- re-radiates the energy at the

same frequency and the scattered X-rays have the same wavelength as the incident beam. No energy absorbed in medium, photon scatters at small angles [Greening 1985].

Pair Production

This process is energetically possible when the photon's energy is $E \geq 1.02\ MeV = 2\ m_o c^2$. The interaction takes place in the Coulomb field of a nucleus. It is possible to take place in the region of an orbital electron. This effect referred as triplet production has a threshold of $4m_0c^2$. The photon disappears and is replaced by an electron-positron pair. Each particle has a mass of $m_0c^2 = 0.511$ MeV. The excess energy over 1.02 MeV goes to kinetic energy shared by the positron and electron. The positron will annihilate after slowing down in the medium, so two annihilation photons with opposite directions are produced as secondary products of the interaction [Greening 1985].

A.5 HALF VALUE LAYER

Half Value Layer

The HVL is defined as the thickness of an absorber which reduces the air-kerma rate of a narrow X-ray beam at a reference point distant mm or cm from the absorbing layer to 50.0% compared with the air-kerma rate for a non attenuated beam.

$$HVL = 0.693 \times \text{Average Range} = 0.693/\mu \quad (2)$$

The HVL is inversely proportional to the attenuation coefficient.

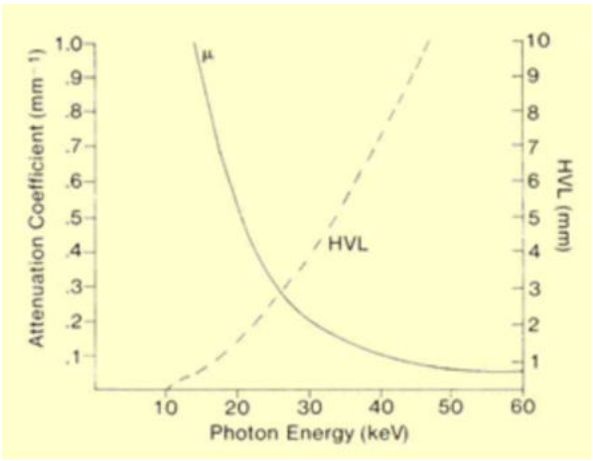

Figure 1. Relationship Between Attenuation Coefficient And HVL For Aluminum. (http://www.sprawls.org)

The figure above shows the HVL and the attenuation coefficient. [Sprawls et al 1995, De Werd et al 1999].

CHAPTER B: *MATERIALS AND METHODS*

B.1 Quality Assurance

Quality Assurance

In the last decades, there has been an extended scientific discussion concerning radiation protection and dosimetry in medical X-ray imaging practice. The presence of different equipment and X-ray practices not only affects the dose of the patients, but the dose of the personnel, as well. The variety of the available equipment and X-ray practices not only affect the dose the patient receives, but also affects the dose received by the personnel. There are several studies regarding (several researchers have concerned the necessary shielding requirements in order to protect the occupational and living areas from the X-ray scatter radiation. Except from shielding calculations, current X-ray practices consider calculation of secondary radiation, in the proximity area to the X-ray tube, as mandatory to be necessary. Such knowledge should be of assistance to technical staff. Such requirements would help technical staff when in performing examinations with mobile radiography units, to medical staff in operating mobile fluoroscopic units, or even to escorts. This study is the measurement of secondary radiation in a conventional radiographic room, in terms of the dose rate, and the study of the influence of different radiographic exposure factors (tube voltage, tube current, distance), with the field size kept constant.

This study can be of importance in optimizing the radiation protection of people and medical personnel, which have to be present in an X-ray room during typical radiography or fluoroscopy procedures. In addition the inclusion of X-ray filtration, as an exposure parameter for 100 kVp tube voltage, can make the presented results applicable to clinical exposure conditions, like coronary angiography, whereby, added filtration and increased tube voltage is utilized for heavy patients. Furthermore, we also conduct a Monte Carlo Simulation analysis, where we simulate the production of the dose rate of secondary radiation [Noto *et al* 2003, Noto *et al* 2009, Vlachos *et al* 2015].

General Considerations

An adequate diagnostic quality assurance (QA) program involves periodic checks of the components in a diagnostic X-ray imaging system. The optimum QA program for any individual facility will depend on a number of factors which include, but may not necessarily be limited to, items such as the type of procedures performed, type of equipment utilized, and patient workload. The program should be developed under the guidance and supervision of a medical physicist qualified in this area of expertise by education, training, and experience. The qualified medical physicist should be involved in close consultation during design, initiation, implementation, and evaluation phases of the program. The medical physicist may be a full-time employee or a consultant to the hospital [Akaagerger et al 2015].

By quality control or quality assurance defined a series of checks and measures aimed at ensuring the good operation of radiographic unit, high quality diagnostic images and the radiation safety of patients and staff. Measurements and controls refer to specific parameters relating to:

1. The X-ray beam quality (Half Value Layer).
2. The geometry of the beam.
3. Radiation output.
4. Performance and good operation of various components and peripherals radiological systems.
5. Image quality.
6. Possible radiation leaks.
7. The electrical and mechanical stability.
8. Electrical Safety.

As has been found, non proper operation of radiological equipment can significantly increase the burden on the patient to radiation (increase of the absorbed dose up to 40-50%). Important is also the increase in operating costs (repeat examination etc).

As part of this work was necessary before we proceed to the measurements ensure the good radiographic tube operation. Since the last official periodic inspections carried out by the Hospital Physicists in that radiography unit (Philips Optimus 80) was used. It is equipped with a three phase high voltage generator, a diagnostic X-ray tube with two focal spots, a tube voltage ranging from 40 to 150 kVp, a tube current ranging from 1 to 660 mA and an exposure time ranging from 0.001 to 16 s. The systems (HVL) was measured 2.1-mm Al at 70 kVp. The19radiography system was installed in the Radiology Department of the Sismanoglio General Hospital of Athens, Greece. The conventional radiographic system, was used since it provided better reproducibility of the measurement set up.

In order to simulate the human head, a cylindrical phantom from plexiglas with a diameter of 16 cm and a height of 15 cm was used [Vlachos et al 2015]. The simple symmetrical shape of the phantom diminished the effect of the phantom shape to the measured scattered radiation shows very good function in relation to the requirements of the Greek Atomic Energy Commission, and the demands of this job. For these checks, used the following instruments:

- PTW- Freiburg, T43014, Diavolt Universal kVp-Dose Meter.
- PTW-Freiburg, DIADOS E, T11035-0260. Detector, DIADOS, T60004, 45-150 kV.
- Fluke Biomedical, 451P-DE-SI-RYR, DEV 2111, Ion Chamber Survey Meter.
- XR-100T-CdTe X-Ray & Gamma Ray Detector.

CHAPTER B: *MATERIALS AND METHODS*

B.2 VALIDATION PARAMETERS

Experimental Setup

A conventional radiographic system (Philips Medio 65 CP-H) was used. It was is equipped with a three phase high voltage generator, a diagnostic X-ray tube with two focal spots, a tube voltage ranging from 40 to 150 kVp, a tube current ranging from 5 to 700 mA and an exposure time ranging from 0.003 to 16 s. The systems (HVL) was measured 3.2-mm Al at 80 kVp. The radiography system was installed in the Radiology Department of the Sismanoglio General Hospital of Athens, Greece [Vlachos *et al* 2015].

In order to simulate the human body, a cylindrical water phantom with a diameter of 38 cm and a height of 20 cm was utilized. The simple symmetrical shape of the phantom diminished the effect of the phantom shape to the measured scattered radiation [Vlachos *et al* 2015].

At the bottom, of the cylindrical water phantom a cross mark was sketched so as to focus the tube's light beam to the mark easily and accurately. It was found that deviations in the focus accuracy, up to 5 cm, did not change the resulting dose rate measurements [Vlachos *et al* 2015].

The ionization chamber used for measuring the secondary radiation was a calibrated 451P-DE-SI model of Fluke Biomedical. This model has been found to can measure the scattered and radiation leakage around the radiographic tubes. Such survey meters have the advantage that they can cover a wide range of photon energies. In this study the irradiation time was kept at 2.5 s so as to account for the response time of the instrument [Le Galley et al 1935, Tsalafoutas et al 2003, 2006]. In order to achieve positioning reproducibility, the survey meter was placed on a photographic stand, with elevating, rotating mechanisms and wheels [Vlachos et al 2015]. Although, the X-ray unit was is subject to periodical quality controls in order to assure its consistency and reproducibility, it was checked prior to the experiments for consistency and reproducibility and was found to be within the acceptable limits. The voltage and irradiation time were checked with a non-invasive X-ray test device (Diavolt Universal of PTW-Freiburg), while the X-ray output was measured with the Diados E dosimeter of PTW-Freiburg, with the radiation semiconductor detector Diados T60004, which is suitable for tube voltages between 45 to 150 kVp. The calibration factors of the T60004 detector are selectable for different X-ray filtration 23 22 and the detection system does not require air density correction with a radioactive check device or measurement of air pressure and temperature [Ramirez-Jime *et al* 2004, Health Physics Society 2014].

The phantom was placed on the radiographic table and irradiated at a stable field size of 40 x 40 cm^2 , and at a stable distance between the tube focal spot and the phantom at 1.0 m. The X-ray field that was utilized was 40 x 40 cm^2, so as to completely cover the cylindrical phantom of 38 cm diameter, and to avoid angular dependence of the results, due to the different self absorption. In addition, the large field size will provide more conservative results and thus provide a worst case scenario which may be of importance in radiation protection issues. The survey meter was placed at a height of 15 cm related to the phantom bottom, with its measuring surface viewing the phantom, as well as, the scattered radiation coming from the unit table and room floor (figure 2) [Vlachos *et al* 2015].

The scatter radiation was measured at different scattering angles around the water phantom (0° to 360°, with a step of 45°) and at distances of 1.0 m, 1.5 m and 2.0 m respectively from the center of the phantom, for different exposure parameters. The height of the survey meter in respect to the bottom of the phantom was kept stable [Vlachos *et al* 2015].

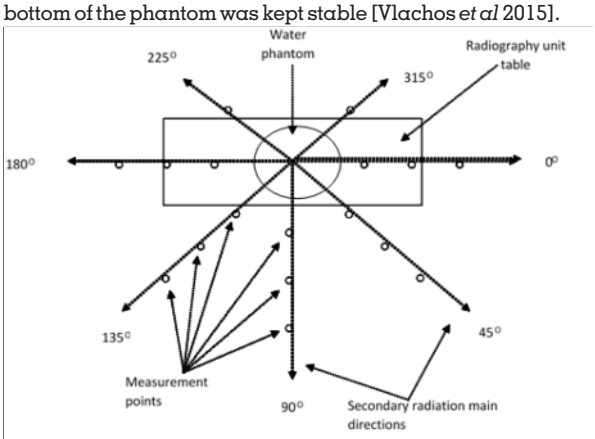

Figure 2. Secondary radiation measurement positions in the radiographic room.

A conventional radiographic system (Philips Optimus 80) was used. It is equipped with a three phase high voltage generator, a diagnostic X-ray tube with two focal spots, a tube voltage ranging from 40 to 150 kVp, a tube current ranging from 1 to 660 mA and an exposure time ranging from 0.001 to 16 s. The systems (HVL) was measured 2.1-mm Al at 70 kVp [Vlachos *et al* 2015]. The radiography system was installed in the Radiology Department of the Sismanoglio General Hospital of Athens, Greece. The conventional radiographic system, was used since it provided better reproducibility of the measurement set up [Vlachos *et al* 2015].

In order to simulate the human head, a cylindrical phantom from plexiglas with a diameter of 16 cm and a height of 15 cm was used. The simple symmetrical shape of the phantom diminished the effect of the phantom shape to the measured scattered radiation. The phantom was placed on the radiographic table and the distance between the phantom and the focus of tube was 83 cm. The distance between the central point of phantom and the point of measuring secondary radiation was 50 cm. The measurement instruments were placed in a special radio protective apparatus and every material was positioned at its input [Vlachos *et al* 2015].

An Amptek XR-100 CdTe spectrometer was used for measuring secondary X-rays and energy distribution. The response of the spectrometer for various energies in terms of energy per bin and detector quantum efficiency per energy value were known through calibration in various radiation energies and published. In X-ray spectrum measurements, the tube voltage was stable at 70 kVp, the tube load was stable at 32 mAs literature [Abbene *et al* 2006, Dos Santos *et al* 2007, Michail *et al* 2011, Martini *et al* 2015, Vlachos *et al* 2015].

The ionization chamber used for measuring the secondary radiation was a calibrated 451P-DE-SI model of Fluke Biomedical. This model can measure the scattered and

radiation leakage around the radiographic tubes. Such, survey meters have the advantage that they can cover a wide range of photon energies. In this study the irradiation time was kept at 2000 ms so as to account for the response time of the instrument. The secondary radiation dose rate (mSv/hr) was measured at a fixed location, with or without a barrier material present [Vlachos *et al* 2015].

The materials which were used as barriers for the secondary X-ray transmission were: a) Single ceramic tile with thickness at 0.7 cm, b) reinforced ceramic tile with thickness at 0.8 cm, c) double reinforced ceramic tile with thickness at 1.8 cm, d) glass block with thickness at 7.9 cm and e) single plasterboard (or gypsumboard wall) with thickness at 1.3 cm and f) double plasterboard with thickness at 2.6 cm. All thickness were measured with a vernier caliper with reading error 0.05 mm [Vlachos *et al* 2015].

Experimental Methodology

The experimental procedure was divided into three parts of measurements. In the first part, the dose rate inside the room was measured for increasing values of the tube current, 10 mA, 25 mA and 50 mA keeping the rest of the exposure factors stable: 100 kVp, 2.5 s [Vlachos *et al* 2015]. The primary beam filtration was inherent. In the second part, the measurements were repeated with an additional filtration of 2 mm-Al at the tube voltage of 100 kVp in order to simulate higher filtered X-ray tubes utilized mainly in interventional radiology procedures for heavy patients [Vlachos *et al* 2015]. Finally, the dose rate was measured for increasing the tube voltage values (60 kVp, 80 kVp and 100 kVp), by keeping the rest of exposure factors stable at 2.5 s and 25 mA. In this case, the primary beam filtration, was again the inherent [Vlachos et al 2015].

We worked with two different irradiation fields, the first was at 7.5 cm x 7.5 cm, to simulate a radiation field of CBCT on the patient head and the second was at 16 cm x 2 cm, to simulate panoramic X-rays. The error of the spectrometer and survey meter placement towards the phantom was never greater than 1 cm and the error of placement concerning the angle with respect to the phantom and the radiographic table was less than 1 degree [Vlachos *et al* 2015]. Tests revealed that the angular errors did not change the measurements much, but the absolute verticality of the survey meter towards the center of the phantom did. In all measuring cases, the experimental procedure was the following: a) the focal spot to the phantom distance was first measured with the tubes and the outer meter, b) the distance from the center of the tubes light spot to the measuring point in the room was measured. Before the measurements a quality control was performed in the radiographic unit to assess its reproducibility and accuracy [Vlachos *et al* 2015].

Uncertainty Of The Measurements

The result of measurement is complete if it is accompanied by a statement of the uncertainty in the measurement. Uncertainties from measurement can come from the instrument, the item being measured, the environment, the operator, and etc [Bell et al 1999]. Uncertainties can be estimated using statistical analysis from set of measurements and from other information about the measurement process. There rules are established for how calculate an overall estimate of uncertainty from these individual pieces of information. Good practice such as traceable calibration, careful calculation, keeping good record, and checking can be reduced by measurement uncertainties [Bell et al 1999]. Uncertainty measurement is evaluated and stated, the fitness for purpose of the measurement can be properly judged. Some situations can undermine the measurement. Flaws in the measurement may be visible or invisible. Real measurements are never made under perfect conditions, uncertainties and errors come from [Bell et al 1999]:

- Measuring instrument/s can suffer from some errors including bias, changes due to ageing, wear, or other kinds of drift and noise.
- The item being measured which may not be stable.
- Process of measurement and the measurement itself may be difficult to do. As example measuring the weight of small animals presents difficulties to co-operate.
- Better' uncertainties calibration of our instrument has an uncertainty which is then built into the uncertainty of the measurements you make.
- The skill of operator, some measurements depend on the skill and judgment of the operator.
- For people could be better than another at the delicate work of setting up a measurement, or at reading fine detail with eye. The use of an instrument such as a stopwatch depends on the reaction of time and the operator [Bell et al 1999].
- About sampling and the measurements that you make, must be properly representative of the process you are trying to assess. About the temperature at
- 26the work-bench, don't measure it with thermometer placed near an air conditioning. Additionally if you are choosing samples from a production line for measurement, don't take the first ten made on a first day morning of the week.
- The temperature and environment, air pressure, humidity and many other conditions can affect the measuring instrument or the item being measured.

Where the size and effect of an error are known (from a calibration certificate) a correction can be applied to the measurement result. In general about uncertainties from each of these sources, and from other sources, would be 'inputs' contributing to the overall uncertainty in the measurement [Bell et al 1999].

Ways to estimate uncertainties:

- Type A evaluations - uncertainty estimates using statistics (usually from repeated readings).
- Type B evaluations - uncertainty estimates from any other information. This could be information from past experience of the measurements, from calibration certificates, manufacturer's specification/s, from the calculation/s, from common sense and from published information [Bell et al 1999].

Coverage Factor K

In this set-up, the survey could measure X-rays scattered from the phantom, the walls, the floor and the ceiling, as well as leakage radiation from the X-ray tube, which was found to be negligible . A systematic study was performed so as to depict the measurement errors due to the measurement set-up. In the measurements, the positioning of the phantom with respect to the X-ray tube and that of the survey meter with respect to the phantom were within 1 cm of marginal error [Vlachos *et al* 2015]. Additionally, the orientation of the survey with respect to the X-ray tube floor axis was within 18 marginal error. The uncertainty of the measurements due to the survey positioning, the phantom positioning, the survey reading error, the survey calibration the survey 27measurements and the repeatability of the X-ray tube output was 6.4%. This reported expanded uncertainty is based on a standard uncertainty multiplied by a coverage factor k = 2, providing a level of confidence 95.0% [Vlachos *et al* 2015].

Energy Distribution Of Scatter Radiation

The X-ray scatter energy distribution (i.e. spectrum) was measured by means of an Amptek XR-100 CdTe spectrometer. The device was placed at 90o angles to the phantom at a distance of 50 cm. The spectrometer was equipped with a collimator with a diameter of 0.2 mm, allowing only scatter X-

rays from the phantom to be measured [Vlachos *et al* 2015].

The correction of the spectrometer with respect to the energy per X-ray bin was equal to (1/5.89) keV, through calibration in various radiations energies. In addition, the correction of the spectrometer with respect to its quantum efficiency (QE) response of the CdTe was obtained from the manufacturer data sheet [Amptek]. The quantum efficiency of the spectrometer shows how effectively the incident X-rays are absorbed in CdTe per energy bin. Q(E) is a function of the X-ray attenuation coefficient per energy. The correction CF(E) per energy to complement X-ray absorption efficiency was

$$CF(E) = 0.000002 * E^3 - 0.0001 * E^2 + 0.008 * E + 1.0362 \quad (3)$$

where E is the X-ray energy and was obtained by considering the X-ray interaction probabilities. CF(E) was multiplied with the detected X-rays photons per energy bin [Dos Santos *et al* 2007, Michail *et al* 2011, Martini *et al* 2015, Vlachos *et al* 2015].

B.3 INSTRUMENTS

PTW- Freiburg, T43014, Diavolt Universal kVp-Dose Meter

Non invasive X-ray meter for kVp, PPV (Practical Peak Voltage), dose and exposure time measurements at X-ray installations [PTW 2015].

- Compact universal meters.
- Measures kV_p, PPV, dose and exposure time in one shot according to IEC 61676.
- Independent of orientation.
- Fast sampling frequency.
- Convenient use for under couch tubes.

The DIAVOLT is designed for measurements of kV_{pmean}, kV_{pmax}, PPV, exposure time and dose of X-ray installations for CT, radiography, fluoroscopy, mammography and for dental applications [PTW 2015]. The key features of the small and light-weight all-in-one device provide easy handling because of automatic functions like auto start, auto stop and auto range. The display reading switches automatically when used for measurements on under couch tubes.

The DIAVOLT has an analogue output which connects to an oscilloscope for displaying the voltage waveform. Furthermore because of the fast sampling frequency, precise measurements can be performed even on very demanding X-ray units with high substantial ripples. No test shots for determination of the right detector orientation are necessary and no external accessories are required for operation. Via the optional DiaControl expert software for automatic data evaluation, quality parameters like the accuracy, reproducibility and linearity can be checked fast a and easily [PTW 2015].

Specifications

Table 1. Specifications Of PTW- Freiburg, T43014,diavolt Universal kVp-Dose Meter.

Type of product	Non invasive kV_p, PPV, dose and time meter
Application	Measurements for acceptance tests and quality control in radiography, fluoroscopy, dental X-ray, CT and Mammography.
Measurements quantities and units	Maximum peak voltage (kV), Mean maximum peak voltage (kV), Practical peak voltage (kV), Dose (Gy, R), RQR, RQR qualities, Irradiation time (s).
Measuring range: Tube voltage Dose Time	(40...150) kV (conventional) (22...40) kV (MAM) 50 µGy...50 Gy (conventional) 150 µGy...150 Gy (conventional) 0.3 ms...999 s
Digital resolution: Tube voltage Dose Time	0.1 kV 0.5 µGy (conventional), 1.5 µGy (MAM) 300 µs
Accuracy: Tube voltage Dose Time	 ≤ ± 1 % or ± 1 kV (conventional) ≤ ± 2 % ≤ ± 0.3 ms
Maximum field size	34 x 34 mm^2 (RAD, FLU, DENT, MAM) 34 x 3 mm^2 (CT, DENT-PANORAMIC)
Range of use: Dose rate Temperature Relative humidity Air pressure	 (1...20) mGy/s (kV measurement) (15...35) °C, (59...95) °F (20...80) %, max. 20 g/m^3 (700...1060) hRa
Display	4-line LCD, automatically display flip
Interface	RS232 and analogue kV waveform
Power supply	4 NiMH batteries (AA) 1.2 V charged by external power supply
Dimensions (H x W x D)	45 mm x 95 mm x 155 mm 1.77 in x 3.74 in x 6.10 in
Weight	Approx. 770 g, 1.70 lbs without batteries

Figure 3. The PTW- Freiburg, T43014, Diavolt Universal kVp-Dose Meter. (http://www.ptw.de)

PTW-Freiburg, DIADOS E, T11035-0260 & Detector, DIADOS, T60004

DIADOS E Diagnostic Dosemeter:

Diagnostic routine dosemeter for QC of radiographic, fluoroscopic, mammographic, dental and CT X-ray installations [PTW 2015].

- Valuable small size dosemeter for acceptance tests and service of any X-ray equipment.
- Measures dose, dose rate, dose per pulse, pulses, dose length product and irradiation time.
- Complies with IEC 61674.
- Includes electrometer modes for current (3 pA to 20 μA) and charge (3 pC to 200 mC) measurement.

The DIADOS E is a small size dosemeter for acceptance tests and routine quality control of any type of diagnostic X-ray installation, which measures dose values and irradiation time. It utilizes semiconductor detectors except for CT measurement, which is based on a pencil ion chamber connected to a separate high voltage supply [PTW 2015]. The calibration factors of the detectors are selectable for different X-ray filtration. The auto-start feature for the dose and exposure time measurement starts as soon as the instrument detects radiation. The measuring ranges in general feature wide dynamics. The automatic zeroing function is another

helpful feature. The DIADOS E can be operated by the mains power supply or by rechargeable batteries. Data can be downloaded from the DIADOS E unit by means of the DiaControl expert software [PTW 2015].

Specifications

Table 2. Specifications of PTW-Freiburg, DIADOS E, T11035-0260. Detector, DIADOS, T60004, 45-150 kV.

Type of product	DIADOS E diagnostic dosemeter for service and acceptance tests.
Application	Dose and dose rate measurements of X-ray installations for radiography, fluoroscopy, mammography, dental X-ray and CT.
Measurements quantities and units	Air kerma (Gy), Air kerma rate (Gy/s), Air kerma length product (Gy·m), Irradiation time (s) Charge (C), Current (A)
Measuring range: Range LOW Range MED Range HIGH	 50 nGy ... 1 Gy 2,0 µGy ... 50 Gy 100 µGy ... 2 kGy
Digital resolution	1 nGy/s resp. 1 nGy
Ranges of use: Detector Type 60004 Detector Type 60005	Detector W-Anode 2.5 mm Al (45 ... 150) kV W-Anode DN3 ... DN10 (45 ... 150) kV W-Anode 8.5 mm Al or W-Anode 8.5 mm Al + 0.8 mm Cu (45 ... 75) kV Mo-Anode 30 µm Mo or Mo-Anode 30 µm Mo + 2 mm Al (25 ... 45) kV
Zero drift	< ± 30 fA
Reproducibility	≤ 0.5 %
Energy	≤ ± 5 % in each of the ranges of use Response
Linearity	≤ ± 2 %
Temperature	(10 ... 40) °C range
Relative humidity	10 % ... 80 %, max. 20 g/m³ range
Air pressure range	(700 ... 1060) hPa
Power supply	4 NiMH batteries (AA) 1.2 V charged by external power supply
Dimensions	180 mm x 100 mm x 45 mm
Weight	Approx. 500 g, with batteries

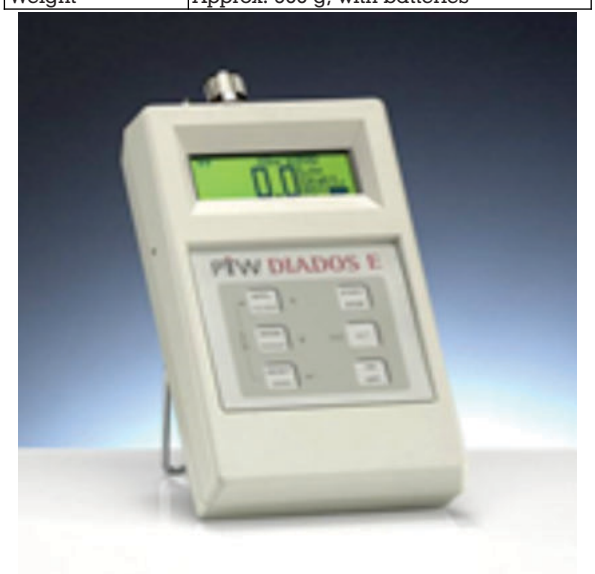

Figure 4. The PTW-Freiburg, DIADOS E Diagnostic Dosemeter. (http://www.ptw.de)

DIADOS / DIADOS E Detectors [PTW]:
Semiconductor detectors for mammography of 25 kV to 45 kV and diagnostic X-rays of 40 kV to 150 kV [PTW 2015].

- Small size and lightweight precision X-ray detectors.
- for acceptance tests and service quality checks.
- Avoid air density corrections with a radioactive check.
- device or measurement of air pressure and temperature.
- Comply with IEC 61674.

The sturdy detectors, supplied with TNC connectors, withstand tough handling. They do not need high voltage supply like ion chambers do. The detector cable length is 2 m. The detectors can measure the following quantities in conjunction with a DIADOS or DIADOS E [PTW 2015]:

- Transmission dose/dose rate behind a phantom.
- Entrance dose/dose rate in the range 40 kV ... 150 kV with and without 25 mm additional Al absorber.
- Dental dose in the range 40 kV ... 90 kV with and without 8.5 mm additional Al filtration.
- Mammography dose in the range 25 kV ... 45 kV with and without 2 mm additional Al filtration.
- Dose per pulse and number of pulses in cinematography or pulsed fluoroscopy.
- Exposure/irradiation time.

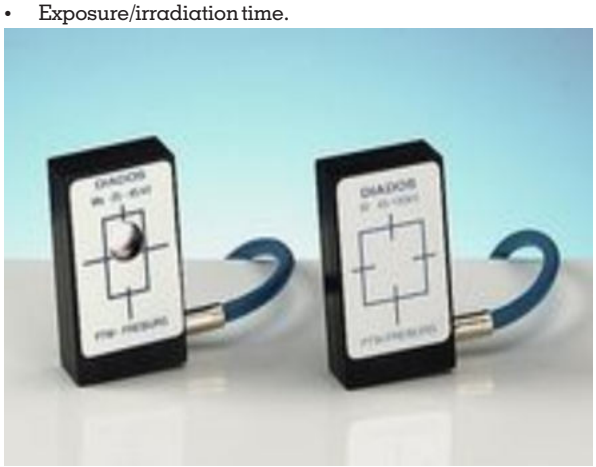

Figure 5. The DIADOS /DIADOS E Detectors. (http://www.ptw.de)

Fluke Biomedical, 451P-DE-SI-RYR, DEV 2111, Ion Chamber Survey Meter

The 451P ion chamber survey meter is a handheld battery operated unit designed for use in both rugged and normal environments. Ideally suited for area monitoring to insure radiation worker safety, the 451P-DE-SI provides precise, mSv, measurements of Deep-Dose Equivalent (ambient dose equivalent, H*(10)) exposure as defined by the United States Nuclear Regulatory Commission and International Commission on Radiation Units & Measurements [Fluke Biomedical 2015]. The 451P auto-ranges and measures radiation rate and accumulated dose from various radiation sources (beta, X-ray and gamma). The ion chamber detector allows for a fast response time to radiation from leakage, scatter beams, and pinholes. Additionally, the low-noise chamber bias supply provides for fast background-settling time. The digital display features an analog bar graph, 2.5 digit readout, low battery indicator, freeze (peak hold) mode indicator and an automatic backlight function. User controls consist of an ON/OFF button and a MODE button [Fluke Biomedical 2015]. The case is constructed of lightweight, high strength materials and is sealed against moisture. The RS-232 interface can be connected directly to a computer for use with the Excel add-in for Windows (451EXL), enhancing the functionality of the instrument [Fluke Biomedical 2015]. This software allows for data retrieval, user parameter selection and provides a virtual instrument display with audible and visual alarm indication [Fluke Biomedical 2015].

Specifications

Table 3. Specifications Of Fluke Biomedical 451P.

Radiation Detected	Beta above 1 MeV & gamma above 25 KeV
Operating Ranges	0 µR/hr to 500 µR/hr (0 µSv/h to 5 µSv/h), 0 mR/h to 5 mR/h (0 µSv/h to 50 µSv/h) 0 mR/h to 50 mR/h (0 µSv/h to 500 µSv/h), 0 mR/h to 500 mR/h (0 mSv/h to 5 mSv/h), 0 R/h to 5 R/h (0 mSv/h to 50 mSv/h)
Accuracy	± 10 % of reading between 10 % and 100 % of full-scale indication on any range, exclusive of energy response (calibration source is 137 Cs)
Detector	230 cc active volume air ionization chamber, pressurized to 8 atmospheres. Plastic chamber wall 200 mg/cm2 thick
Warm-Up Time	Less than one minute for initial operation when the instrument is in temperature equilibrium with the surrounding area and about 4 minutes for readings less than 20 µR/h in a 10 µR/h or less background.
Drift	After seven minutes operation, 0.04 mR/h equivalent, or less
Response Time	Time measured from 10 % to 90 % of final value for a step increase/decrease in radiation rate such that a range change does not occur: 0 µR/h to 500 µR/h (0 µSv/h to 5 µSv/h) range: 5 seconds. 0 mR/hr to 5 mR/hr (0 µSv/h to 50 µSv/h) range: 2 seconds. 0 mR/h to 50 mR/h (0 µSv/h to 500 µSv/h) range: 1.8 seconds. 0 mR/h to 500 mR/h (0 mSv/h to 5 mSv/h) range: 1.8 seconds. 0 R/h to 5 R/h (0 mSv/h to 50 mSv/h) range: 1.8 seconds. NOTE: In pulsating field, the instantaneous rate should not exceed 5 R/h for proper integration; instantaneous exposure rate is still limited to 5 R/h
Precision	Within 5 % reading
Readout	Liquid Crystal Display: contains an analog bar graph with a permanent scale on the display and a 2½ digit display. Analog Display: the bar graph consists of 100 segments, 2½ inches long; the scale has five major divisions; the appropriate value for the operating range of the instrument will appear below the scale. Digital Display: the digital display is 2½ digits followed by a significant zero digit depending on the operating range of the instrument. The leading ½ digit is blank, or a "1" or a "0" for clarity. Units of measure appear to the right of the digital display. Appropriate multipliers also appear on the display Units: as indicated under Range, programmable in R/h or Sv/h. Appropriate multipliers also appear on the display. Auto-On Backlight: turns on when ambient light is less then twilight conditions.
External Controls	ON/OFF button, MODE button
Automatic Features	Ranging and zeroing are fully automatic.
Environmental	Operating Temperature Range: -4 °F to +122 °F (-20 °C to +50 °C) Relative Humidity Range: 0 % to 95 %, non-condensing Geotropism: less than 1 % Altitude 2000 m For Indoor Use
Dimensions (L x W x H)	8.5 in x 4.5 in x 8.6 in (21 cm x 11.4 cm x 21.3 cm)
Weight	Approximately 2.6 lb (1.2 kg)
Batteries	Two 9-volt batteries (NEDA 1604A or 6LR61 or 6AM6) provide over 200 hours continuous operation.

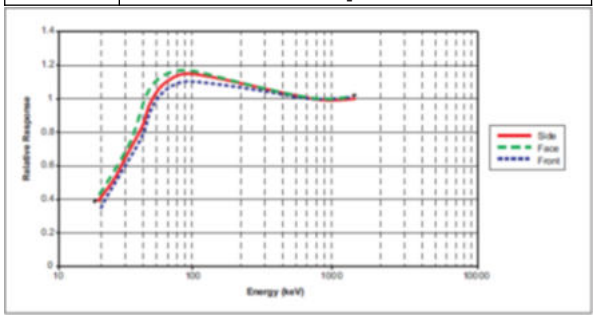

Figure 6. Model 451 P Typical Energy Response. (fluke Biomedical)

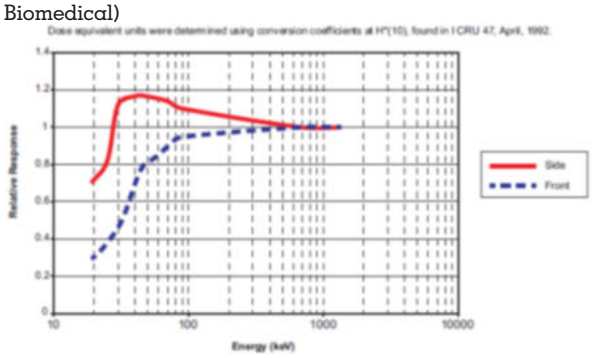

Figure 7. Model 451 P Typical Energy Dependence. (Fluke Biomedical)

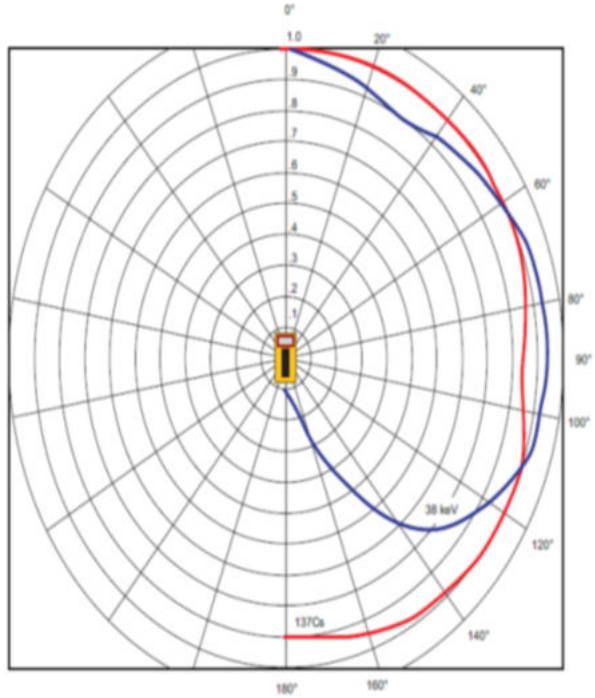

Figure 8. Survey Meter Angular Response. (fluke Biomedical)

Figure 9. The 451P ion chamber survey meter. (http://www.grainger.com/product/FLUKE-BIOMEDICAL-Pressurized-uR-Ion-Chamber-5NLL1)

Amptek XR-100T-CdTe X-Ray & Gamma Ray Detector

The Amptek PX4 is an interface between Amptek's XR100 series of X-ray and γ-ray detectors and a personal computer with data acquisition, control, and analysis software. The PX4 includes three major components: (1) a shaping amplifier, based on a state of the art, high performance, low power DP4 digital pulse processor, (2) a multichannel analyzer, and (3) power supplies. It replaces both the previous generation PX2 shaping amplifier and power supply and the separate MCA. The pulse processing and MCA function of the PX4 are based on Amptek's DP4 digital pulse processor [Amptek 2015]. The PX4 offers several performance advantages over traditional analog systems, including higher energy resolution, reduced ballistic deficit, higher throughput, better pile-up rejection, enhanced stability, and the ability to adjust shaping time parameters over a wide range to optimize performance. The PX4 includes a USB interface. The power supply portion of the PX4 provides all of the power necessary for the detector, preamplifier, and the PX4. The PX4 offers several advantages: (1) a single unit interfaces with all XR100 variants, (2) many parameters may be adjusted to optimize performance, such as shaping time constant and HV bias, (3) the pulse processor offers enhanced baseline stability, throughput, pile-up rejection, and Rise Time Discrimination (RTD) and (4) the MCA is integrated with the complete system [Amptek 2015].

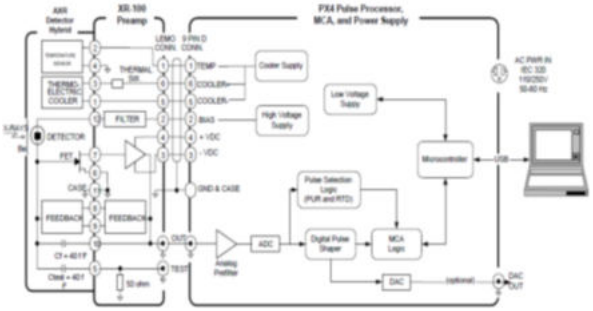

Figure 10. Block Diagram Of The PX4 In A Complete System. (amptek)

The signal input to the PX4 is the preamplifier output. The PX4 digitizes the preamplifier output, applies real-time digital processing to the signal, detects the peak 41.

40amplitude (digitally), and bins this value in its histogramming memory, generating an energy spectrum. The use of digital signal processing offers several important performance advantages compared to previous systems. The spectrum is then transmitted over the PX4's USB interface to the user's computer. The PX4 hardware is controlled over the USB interface, permitting the user not only to start and stop acquisition but to select shaping times, select the HV bias, etc [Amptek 2015].

Specifications

Table 4. Specifications Of Amptek XR-100T-CdTe.

Gain Settings	28 user selectable gain settings from x4 to x550. Fine gain is adjustable between 0.75 and 1.25.
Pulse Shape	Trapezoidal. A semi-gaussian amplifier with shaping time τ has a peaking time of 2.2 τ and is comparable in performance with the trapezoidal shape of the same peaking time.
Peaking and Flat Top Times	Twenty-four programmable peaking times between 0.8 and 102 μsec. For each peak time, sixteen flat top durations are available > 0.2 μsec.
Rise Time Discriminator (RTD)	The digital pulse processor can be programmed to select input pulses based on their rise time properties.
Throughput	The pulse processing electronics have a cycle time of 1 μsec. With a peaking time of 0.8 μsec, a 1MHz periodic signal can be acquired. Dead time is 1.25 x peaking time.
Pile-Up Reject	Pulses separated by more than the fast channel resolving time, 600 nsec, and less than 1.25 x peaking time are rejected.
Number of channels	Command able to 256, 512, 1 k, 2 k, 4 k or 8 k channels.
Analog Input (BNC)	The analog input accepts pulses from the XR100 or any other detector with preamplifier reset or resistive feedback.
XR100 Power (6 pin LEMO)	Provides power to preamp and detector. Includes HV bias, thermoelectric cooler power, and preamp power.
Serial Interface (USB)	Standard USB interface and RS-232 interface to personal computer. Used for data acquisition and hardware control.
DAC Output (BNC)	This output is used in oscilloscope mode, to view the shaped pulse and other diagnostic signals. Range: 0 to 1 V.
Input Power	5 VDC (500 mA max) via power jack. It mates with a center positive 5.5 mm x 2.1 mm Power Plug.

Figure 11. The Amptek XR-100T-CdTe X-Ray & Gamma ray detector. (http://www.directindustry.com/prod/amptek-inc/product-21695-392529.html)

CHAPTER C: *RESULTS AND DISCUSSION*

C.1 VALIDATION

Quality Control Results Of The Radiographic Tubes

For conventional radiographic system (Philips Medio 65 CP-H) measurements showed that a set-up difference of the focal spot to the phantom distance up to 2 cm did not practically affect the measured secondary radiation values. Deviations of the survey meter placement towards the phantom were < 1 cm and did not affect the results [Vlachos et al 2015]. The absolute verticality of the survey meter was kept constant by means of a photographic stand. The total filtration of the X-ray beam was calculated by measuring the HVL. The measured HVL and the X-ray output in terms of milligray per milliampere-second for the tube voltages under investigation are presented in the first three columns of Table 5, for tube current of 25 mA. It can be observed that HVL varies between 2.7-mm Al and 4.6-mm Al, well inside typical HVL values [Vlachos et al 2015].

For conventional radiographic system (Philips Optimus 80), the accuracy of the X-ray tube voltage was 1.3%, and its reproducibility was 1.9%. The measurements were performed with the PTW-Freiburg 43014, Diavolt Universal kVp-Dose-time meter placed at a distance of 1.0 m from the focal spot on the upper surface of the cylindrical phantom. The tube voltage deviation from the theoretical data was taken into account during the measurements. When exposure time was considered both accuracy and reproducibility were better than 0.2% [Vlachos et al 2015].

C.2 DOSE RATE RESULTS & ANALYSIS OF SPECTROMETER DATA

Dose Rate Results And Analysis Of Spectrometer Data

In Table 5 the measured secondary radiation dose rate is shown. The dependence of scatter radiation dose rate from the X-ray tube voltage used was found to follow the equation: $(mSv/h) = 2 \cdot 10^{-7} \cdot (kVp)^{3.853}$, with $R^2 = 0.995$. In addition in Table 5 the dose rate per unit tube current (mSv/h/mA), for 25 mA tube current, is demonstrated [Vlachos *et al* 2015]. These results can be of value for an estimation of H*(10), for various X-ray tube voltages and 2.5 s exposure time, provided the X-ray output and H*(10) is linear with respect to mA. A more detailed account regarding the measured dose rate can be observed in Table 6, where the dose rate for the X-ray tube voltages at 60 kVp, 80 kVp and 100 kVp, with irradiation conditions of 25 mA and 2.5 s is demonstrated, for distances of 1.0 m, 1.5 m and 2.0 m from the phantom. It is interesting to notice that at 315° at distance of 1.0 m, the dose rate increases significantly compared to the other angles [Vlachos *et al* 2015]. In Table 7, the corresponding results for the 100 kVp with an additional 2.0-mm Al filtration are shown. It can be observed that the dose rates are lower in respect to the 100 kVp tube voltage and the same exposure conditions. The proportionality of dose rate with mA is verified. This behavior was also observed in the case of no additional filtration measurements.

The inclusion of X-ray filtration, as an exposure parameter for 100 kVp tube voltage, can make the presented results applicable in clinical conditions such as coronary angiography, where added filtration and increased tube voltage are utilized for obese patients. Figure 12 shows the scatter radiation X-ray energy distribution. Due to the collimator of the Amptek spectrometer these measurements do not consider neither secondary radiation from the floor, the walls and the ceiling, nor leakage radiation from the X-ray tube. The average energies of the spectra correspond to 34.88 keV, 48.80 keV, 68.44 keV and 68.45 keV for tube voltages 60 kVp, 80 kVp, 100 kVp and 100 kVp with 2-mm Al additional filtration, respectively. The corresponding mode energy values were 34.0 keV, 45.0 keV, 81.0 keV and 71.0 keV. The average and mode energies might be of value for personnel dosimeter calibration purposes [Vlachos *et al* 2015].

Table 5. The X-ray output, the X-ray beam HVL, the secondary dose rate and the dose rate per tube current for various tube voltages at 1.5 m, at 90o angle and 25 mA and 2.5 s.

Tube voltage(kVp)	X-ray output (mGy/mAs)	Calculated HVL (mm-Al)	Secondary radiation dose rate at 1.5 m, at 90o angle (mSv/hr)	Dose rate normalized at 25mA (mSv/hr)/mA)
60	0.04	2.7	1.2	0.048
80	0.09	3.2	4.1	0.164
100	0.15	3.7	8.5	0.34
100 (+2.0 mmAl)	0.10	4.6	7.0	0.28

Table 6. Secondary Radiation Dose Rate With No Added Filtration For Various Distances, Tube Voltages And Angles At 25 mA Tube Current And 2.5 s Exposure Time.

Angle of scattered radiation (degrees)		0°	45°	90°	135°	180°	225°	315°
Distance from the phantom (m)	Tube Voltage (kVp)	Secondary radiation dose rate (mSv/hr)						
1.0	100	19.0	19.0	18.5	19.5	18.5	18.5	22.0
1.5	100	8.0	8.0	8.5	8.0	8.0	-	-
2.0	100	4.5	4.9	4.5	4.9	4.9	-	-
1.0	80	8.5	8.0	8.5	8.0	8.0	8.5	9.5
1.5	80	4.0	3.8	4.1	3.9	3.9	-	-
2.0	80	2.3	2.3	2.5	2.3	2.3	-	-
1.0	60	2.5	2.5	2.6	2.4	2.4	2.5	2.8
1.5	60	1.1	1.1	1.2	1.1	1.1	-	-
2.0	60	0.7	0.7	0.7	0.6	0.6	-	-

Table 7. Secondary Radiation Dose Rate With An Additional Filter Of 2-mm Al At 100 kVp For Various Distances, Tube Currents And Angles At 2.5s Exposure Time.

Angle of scattered radiation (degrees)		0 °	45°	90°	135°	180°	225°	315 °
Distance from the phantom (m)	Tube Current (mA)	Secondary radiation dose rate (mSv/hr)						
1.0	10	5.5	5.5	5.5	6.0	5.5	5.5	6.5
1.0	25	15.5	15.5	15.0	16.0	15.0	15.5	18.0
1.0	50	33.5	33.0	32.5	33.5	32.5	33.0	36.0
1.5	10	2.8	2.8	3.0	2.7	2.9	-	-
1.5	25	6.5	6.5	7.0	6.5	7.0	-	-
1.5	50	14.0	14.5	15.0	14.5	14.5	-	-
2.0	10	1.7	1.7	1.7	1.7	1.7	-	-
2.0	25	4.3	4.1	4.3	4.2	4.2	-	-
2.0	50	8.0	8.0	8.0	8.0	8.0	-	-

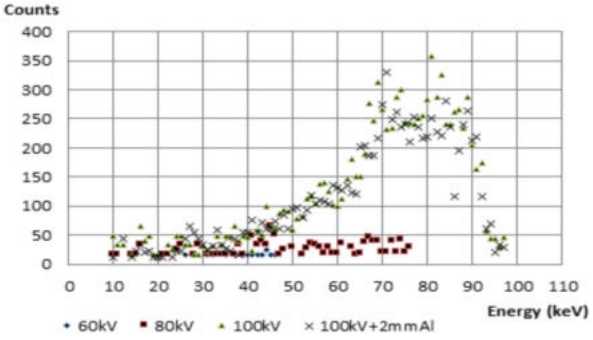

Figure12. Secondary Radiation Energy Distribution For Various X-ray Tube Voltages, Measured At 90° Angle At A Distance Of 50 Cm From The Phantom At 45 mAs.

In figure 13 we can seen the secondary radiation dose rate in each irradiation field with keeping stable 70 kVp, 10 mA, and 2000 ms. At 7.5 cm x 7.5 cm irradiation field, the secondary radiation behind the glass block was 0.1008 mSv/hr, lower than the other materials. At 16 cm x 2 cm irradiation field, the secondary radiation of glass block was 0.1 mSv/hr, lower than the other materials [Vlachos *et al* 2015].

In figures 14 we observe all the spectra of energy distribution at 70 kVp with and without materials at 7.5 cm x 7.5 cm irradiation filed. From figures we can say, that the spectrum of single and reinforced in thickness ceramic tile are almost the same. The double reinforced in thickness ceramic tile (figure 14d), the glass block (figure 14e) and the double plasterboard (figure 14g) was better for radioprotection than others materials.

In figures 15 we observed the energy distribution at the same kVp with and without material, for the irradiation field of 16 cm x 2 cm. All ceramic tiles reduce significantly the spectrum of 70 kVp. The double reinforced in thickness ceramic tile (figure 15d), the glass block (figure 15e) and the double plasterboard (figure 15g) demonstrated higher attenuation properties [Vlachos *et al* 2015].

In addition in table 8 the mean energies of the transmitted spectra are demonstrated as well as, the secondary radiation dose rate is demonstrated. We can observe by table 1 for the 7.5 cm x 7.5 cm irradiation field, that the most higher mean energy value has the single plasterboard at 45.87 keV. Furthermore the mean energies of the single ceramic tile and the reinforced in thickness ceramic tile were 45.86 keV and 45.34 keV respectively. The mean energies at 16 cm x 2 cm irradiation field were higher for the double reinforced in thickness ceramic tile [Vlachos *et al* 2015].

There is a raise in the mean energy of the transmitted X-rays, due to the beam hardening effect produced by the materials. The higher density of the material shifts the attenuated X-ray spectra to higher values, since high density materials tends to absorb more efficiently the low energy part of the spectrum with photoelectric effect. The behaviour of the transmitted secondary radiation in terms of beam hardening was similar to the 16 cm x 2 cm. However in this field, the corresponding mean energy were lower than the 7.5 cm x 7.5 cm irradiation field. This behaviour may be attributed to the increase percentage of scattered X-rays photons due: a) The increased field size facing the detector (16 cm over 7.5 cm), b) the probable scatter contribution by the collimator at the 2 cm dimension, which can be more easily detected by the spectrometer in current geometry or c) by the relative contribution of multiple scattering from photons emission from depths away of the detectors, of the 7.5 cm x 7.5 cm related to the 16 cm x 2 cm irradiation field [Vlachos *et al* 2015].

From table 9 and 10, we can seen the secondary radiation dose rate (mSv/hr) in each irradiation field with keeping stable kVp, mA, and ms. At 7.5 cm x 7.5 cm irradiation field, the secondary radiation behind the glass block was 100.8 □Sv/hr, lower than the other materials, with a transmission of 11.2%. At 16 cm x 2 cm irradiation field, the secondary radiation of glass block was 100.0 □Sv/hr, lower than the other materials, with a transmission of 30.0%. In the same irradiation field, double plasterboard and double reinforced in thickness ceramic tile have similar transmission 30.0%. The air KERMA measured at 2.1 mGy for 7.5 cm x 7.5 cm irradiation field and for 16 cm x 2 cm irradiation field measured at 0.49 mGy [Vlachos *et al* 2015].

The simplest method for determining the effectiveness of the shielding material is using the concepts of half-value layers (HVL) and tenth-value layers (TVL). One half-value layer is defined as the amount of shielding material required to reduce the radiation intensity to one-half of the unshielded value.

$$\mathbf{HVL = \ln 2 / \mu = 0.693 / \mu \quad (4)}$$

The symbol μ is known as the linear attenuation coefficient. One tenth-value layer is defined as the amount of shielding material required to reduce the radiation intensity to one-tenth of the unshielded value [Bushberg *et al* 2001].

$$\mathbf{TVL = \ln 10 / \mu = 2.3026 / \mu \quad (5)}$$

From table 11, we can see the calculations of HVL and TVL in each irradiation field with keeping stable kVp, mA, and ms. The most higher value for HVL and TVL in each irradiation has the glass block [Vlachos et al 2015].

For 16 cm x 2 cm irradiation field our results showed that common building materials may be in value for shielding proposes, especially in the case of low workload and protections room with small occupancy factor [Vlachos *et al* 2015].

Table 8. Irradiation Filed 7.5 Cm X 7.5 Cm And 16 X 2 Cm. Mean Value Of Energy (keV) Of All Materials.

	Irradiation filed 7.5 cm x 7.5 cm	Irradiation filed 16 cm x 2 cm
Without material	39.57	37.31
Single plasterboard	45.87	40.09
Single ceramic tile	45.86	39.63
Reinforced in thickness ceramic tile	45.34	39.85
Double reinforced in thickness ceramic tile	42.39	41.58
Double plasterboard	43.00	41.54
Glass block	42.13	41.45

Table 9. Irradiation Filed 7.5 Cm X 7.5 Cm. With All Materials, With Stable kV, mA, ms. Secondary Radiation Dose Rate Measured For All Materials.

Irradiation field 7.5 cm x 7.5 cm					
	Tube voltage (kVp)	Tube Current (mA)	Irradiation time (ms)	Secondary radiation dose rate	Transmission %
Without material	70	10	2000	0.9 (mSv/hr)	-
Glass block	70	10	2000	100.8 (μSv/hr)	11.2
Double reinforced in thickness ceramic tile	70	10	2000	200.4 (μSv/hr)	22.2
Double plasterboard	70	10	2000	200.5 (μSv/hr)	22.2
Reinforced in thickness ceramic tile	70	10	2000	300.4 (μSv/hr)	33.3
Single ceramic tile	70	10	2000	300.5 (μSv/hr)	33.3
Single plasterboard	70	10	2000	400.4 (μSv/hr)	44.4

Table 10. Irradiation Filed 16 cm x 2 cm. With All Materials, With Stable kV, mA, ms. Secondary Radiation Dose Rate

Measured For All Materials.

Irradiation field 16 cm x 2 cm					
	Tube voltage (kVp)	Tube Current (mA)	Irradiation time (ms)	Secondary radiation dose rate	Transmission %
Without material	70	10	2000	0.5 (mSv/hr)	-
Glass block	70	10	2000	100.0 (µSv/hr)	20.0
Double plasterboard	70	10	2000	150.0 (µSv/hr)	30.0
Double reinforced in thickness ceramic tile	70	10	2000	150.0 (µSv/hr)	30.0
Reinforced in thickness ceramic tile	70	10	2000	200.3 (µSv/hr)	40.0
Single ceramic tile	70	10	2000	200.4 (µSv/hr)	40.1
Single plasterboard	70	10	2000	300.0 (µSv/hr)	60.0

Table 11. HVL And TVL Calculations For All Materials With Respect Of 7.5 cm x 7.5 cm And 16 cm x 2 cm Irradiation Field.

	Irradiation filed 7.5 cm x 7.5 cm		Irradiation filed 16 cm x 2 cm	
Materials	HVL (cm)	TVL (cm)	HVL (cm)	TVL (cm)
Single ceramic tile	4.38	14.57	5.33	17.71
Reinforced ceramic tile	5.02	16.68	6.07	20.19
Double reinforced ceramic tile	8.34	27.74	10.5	34.88
Glass block	25.66	85.28	34.65	115.12
Single plasterboard	11.00	35.54	17.76	59.04
Double plasterboard	12.15	40.39	15.06	50.05

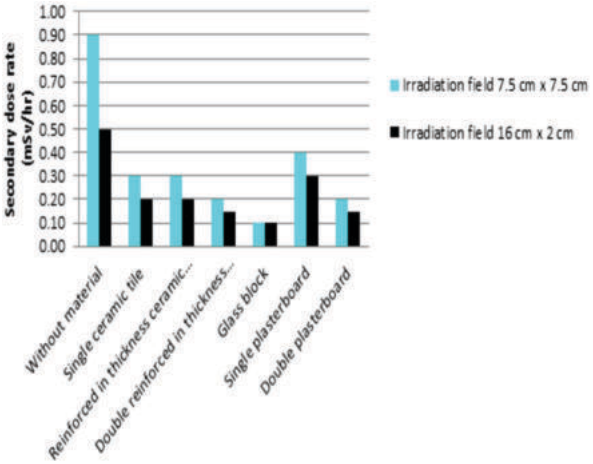

Figure 13. Irradiation Field 7.5 cm x 7.5 cm And 16 cm x 2 cm. Secondary Radiation Dose Rate Measured For All Materials With Stable kV, mA, ms.

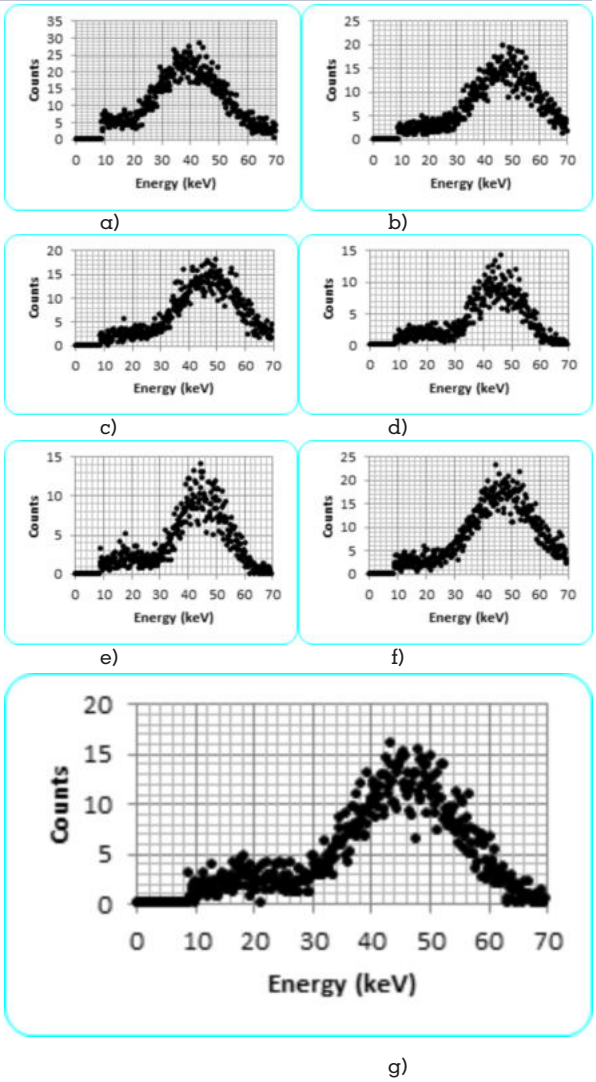

Figure 14. Spectra of energy distribution at 70 kVp, with respect of 7.5 cm x 7.5 cm irradiation field. a) Without material, b) Single ceramic tile, c) Reinforced ceramic tile, d) Double reinforced ceramic tile, e) Glass block, f) Single plasterboard, g) Double plasterboard.55

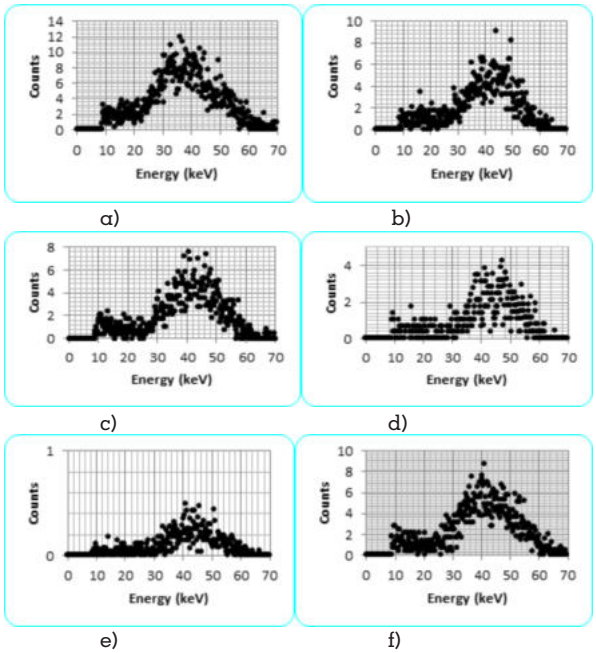

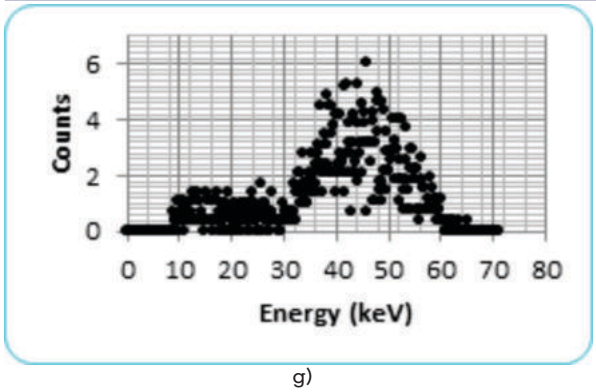

g)

Figure 15. Spectra of energy distribution at 70 kVp, with respect of 16 cm x 2 cm irradiation field. a) Without material, b) Single ceramic tile, c) Reinforced ceramic tile, d) Double reinforced ceramic tile, e) Glass block, f) Single plasterboard, g) Double plasterboard.

CHAPTER D: *CONCLUSIONS AND FUTURE WORK*

D.1 CONCLUSIONS

The decrease of the dose rate in air is larger than 40%, for every half meter away from the phantom, while its angular distribution remained almost stable, given the symmetry of the phantom. The added filtration of 2.0-mm Al further reduced the secondary dose rate 21.4%, due to the related decrease of the X-ray tube output. Finally, if our results were normalized per tube current, i.e. (mSv/hr)/(mA), could be of value for medical staff during mobile X-ray radiography [Vlachos *et al* 2015].

The radio protection in dental and veterinary radiology, testing common building materials such as, ceramic tiles, glass block and plasterboard, of the photon energy spectrum and the secondary diagnostic X-rays. Results showed that the secondary radiation and the energy spectrum are different, using different irradiation fields. It has been shown the secondary radiation and the dose rate (mSv/hr) was reduced at 16 cm x 2 cm irradiation field with respect to the 7.5 cm x 7.5 cm irradiation field. In addition the average transmitted X-ray energy and the dose area was reduce in 16 cm x 2 cm irradiation field compared to 7.5 cm x 7.5 cm irradiation field. In both irradiation fields, the glass block at first and then, the double reinforced in thickness ceramic tile and the double plasterboard provided lower transmission (%) and better radiation protection, from any other common building material for low energies [Vlachos et al 2015].

D.2 FUTURE WORK

Future Work

It is essential to make accurate estimates of the scatter of radiation from the human body when calculating the leakage dose in medical X-ray imaging facilities. The scatter fraction varies with the size and shape of the radiation field in a way that is not exactly proportional to the area of the field [Noto et al 2003, Noto et al 2009]. An important part of determining the radiation protection requirements during X-ray room design is the calculation of the amount of scatter inside and outside the planned locations of the shielding barriers. A Monte Carlo code has been developed to calculate the percentage scatter so that the current data can be consolidated and new data can be provided as required. Calculations have been compared with measurements to show that they are representative of scatter found in X-ray rooms. Scatter from the dose–area product meter and the collimator system were found to provide large contributions to the measured scatter [Mc Vey et al 2004].

Another part that needs to be furthermore investigated is the determining the materials for radio protection proposes and thickness of the shielding material, such as lead, concrete, or gypsum wallboard [Radiation Protection in Dentistry 1999] and other new materials required to reduce radiation levels to the recommended dose limits can be determined through calculations. In general, the radiation exposure to individuals depends primarily on the amount of radiation produced by the source, the distance between the exposed person and the source of the radiation, the amount of time that an individual spends in the irradiated area, and the amount of protective shielding between the individual and the radiation source.

APPENDIX I
ABBREVIATIONS

ALARA	As Low As Reasonably Achievable
CBCT	Cone Beam Computer Tomography
CF(E)	Correction factor
CT	Computer Tomography
FLU	Fluoroscopy
Gy	Gray
ICRP	International Commission on Radiological Protection
ICRU	International Commission on Radiation Units & Measurements
H*(10)	Ambient Dose Equivalent
HVL	Half Value Layer
k	Coverage factor
KERMA	Kinetic Energy Released per unit Mass
MAM	Mammography
MCA	Multi channel analyzer
PPV	Practical Peak Voltage
Q(E)	Attenuation coefficient per energy
QA	Quality assurance
QE	Qantum efficiency
R	Roentgen
RTD	Rise Time Discrimination
SI	International System
STP	Standard temperature and pressure
Sv	Sievert
TVL	Tenth Value Layer
Elements:	
Al	Aluminium
CdTe	Cadmium telluride

APPENDIX II
LIST OF FIGURES

Figure 1. Relationship between attenuation coefficient and HVL for Aluminum. (http://www.sprawls.org)

Figure 2. Secondary radiation measurement positions in the radiographic room.

Figure 3. The PTW- Freiburg, 43014, Diavolt Universal kVp-Dose Meter. (http://www.ptw.de)

Figure 4. The PTW-Freiburg, DIADOS E Diagnostic Dosemeter. (http://www.ptw.de)

Figure 5. The DIADOS /DIADOS E Detectors. (http://www.ptw.de)

Figure 6. Model 451 P Typical energy response. (Fluke Biomedical)

Figure 7. Model 451 P Typical energy dependence. (Fluke Biomedical)

Figure 8. Survey meter angular response. (Fluke Biomedical)

Figure 9. The 451P ion chamber survey meter. (http://www.grainger.com/product/FLUKE-BIOMEDICAL-Pressurized-uR-Ion-Chamber-5NLL1)

Figure 10. Block diagram of the PX4 in a complete system. (Amptek)

Figure 11. The Amptek XR-100T-CdTe X-Ray & Gamma Ray Detector. (http://www.directindustry.com/prod/amptek-inc/product-21695-392529.html)

Figure12. Secondary radiation energy distribution for various X-ray tube voltages, measured at 90° angle at a distance of 50 cm from the phantom at 45 mAs.

Figure 13. Irradiation field 7.5 cm x 7.5 cm and 16 cm x 2 cm. Secondary radiation dose rate measured for all materials with stable kV, mA, ms.

Figure14. Spectra of energy distribution at 70 kVp, with

respect of 7.5 cm x 7.5 cm irradiation field. a) Without material, b) Single ceramic tile, c) Reinforced ceramic tile, d) Double reinforced ceramic tile, e) Glass block, f) Single plasterboard, g) Double plasterboard.

Figure15. Spectra of energy distribution at 70 kVp, with respect of 16 cm x 2 cm irradiation field. a) Without material, b) Single ceramic tile, c) Reinforced ceramic tile, d) Double reinforced ceramic tile, e) Glass block, f) Single plasterboard, g) Double plasterboard.

APPENDIX III

LIST OF TABLES

Table 1. Specifications of PTW- Freiburg, 43014, Diavolt Universal kVp-Dose Meter.

Table 2. Specifications of PTW-Freiburg, DIADOS E, T11035-0260. Detector, DIADOS, 60004, 45-150 kV.

Table 3. Specifications of Fluke Biomedical 451P.

Table 4. Specifications of Amptek XR-100T-CdTe.

Table 5. The X-ray output, the X-ray beam HVL, the secondary dose rate and the dose rate per tube current for various tube voltages at 1.5 m, at 90° angle and 25mA and 2.5 s.

Table 6. Secondary radiation dose rate with no added filtration for various distances, tube voltages and angles at 25 mA tube current and 2.5 s exposure time.

Table 7. Secondary radiation dose rate with an additional filter of 2 mm-Al at 100 kVp for various distances, tube currents and angles at 2.5 s exposure time.

Table 8. Irradiation filed 7.5 cm x 7.5 cm and 16 x 2 cm. Mean value of energy (keV) of all materials.

Table 9. Irradiation filed 7.5 cm x 7.5 cm. With all materials, with stable kV, mA, ms. Secondary radiation dose rate measured for all materials.

Table 10. Irradiation filed 16 cm x 2 cm. With all materials, with stable kV, mA, ms. Secondary radiation dose rate measured for all materials.

Table 11. HVL and TVL calculations for all materials with respect of 7.5 cm x 7.5 cm and 16 cm x 2cm irradiation field.

SUMMARY

The aim of this thesis, is the measurement of secondary radiation in a conventional radiographic room, in terms of the dose rate, and the study of the influence of different radiographic exposure factors (tube voltage, tube current, distance), with the field size kept constant. This thesis can be of importance in optimizing the radiation protection of people and medical personnel, which have to be present in an X-ray room during typical radiography or fluoroscopy procedures. In addition the inclusion of X-ray filtration, as an exposure parameter for 100 kVp tube voltage, can make the presented results applicable to clinical exposure conditions, like coronary angiography, whereby, added filtration and increased tube voltage is utilized for heavy patients. Except from shielding calculations, current X-ray practices consider calculation of secondary radiation, in the proximity area to the X-ray tube, as mandatory to be necessary.

Such knowledge should be of assistance to technical staff. Such requirements of this thesis are of value during exposure of people not protected by shielding materials such as radiographers, and patients during the use of mobile X-ray units, since it has demonstrated that the choice of the tube voltage and filtration affects of the dose rate from the scatter radiation.

In the first experimental, it was found that the dose rate decrease in air is larger than 40.0%, for every half meter away from the phantom, while its angular distribution remained almost stable given the symmetry of the phantom. The added filtration of 2.0 mmAl, further reduced the scattered dose rate by 21.4%, because of the related decrease in the X-ray tube output. These results can be of value for an estimation of ambient dose rate equivalent H*(10), for various X-ray tube voltages and 2.5 s exposure time, provided the X-ray output and H*(10) is linear with respect to mA. A more detailed account regarding the measured dose rate can be observed in Table 6, where the dose rate for the X-ray tube voltages at 60, 80 and 100 kVp, with irradiation conditions of 25 mA and 2.5 s is demonstrated, for distances of 1.0, 1.5 and 2.0 m from the phantom. It is interesting to notice that at 315° at distance of 1.0 m, the dose rate increases significantly compared to the other angles. In Table 10, the corresponding results for the 100 kVp with an additional 2.0 mmAl filtration are shown. It can be observed that the dose rates are lower in respect to the 100 kVp tube voltage and the same exposure conditions. The proportionality of dose rate with mA is verified.

Dental and veterinary radiography is one of the most valuable tools used in modern dental health care. It enables the diagnosis of physical conditions that would otherwise be difficult to identify, and thus, its judicious use is of considerable benefit to the patient. However, the use of dental radiological procedures must be carefully managed, because radiation has the potential for damaging cells and tissues. The aim of radiation protection in dentistry and veterinary is to obtain the desired clinical information with minimum radiation exposure to patients, dental and veterinary personnel, and the public. The most popular material for radio protection is lead, however it is known to be toxic and expensive. For these reasons it might be interest to use common building materials, such as a) single ceramic tile, b) reinforced ceramic tile, c) double reinforced ceramic tile, d) glass block, e) single plasterboard (or gypsumboard wall) and f) double plasterboard, for radiation protection especially to adjacent areas, where small thicknesses of lead may be required and the workload of the equipment is small.

In the second experimental showed that the secondary radiation and the energy spectrum are different, using different irradiation fields. It has been shown the secondary radiation and the dose rate (mSv/hr) was reduced at 16 cm x 2 cm irradiation field with respect to the 7.5 cm x 7.5 cm irradiation field. At 16 cm x 2 cm irradiation field, the secondary radiation of glass block was 100.0 Sv/hr, lower than the other materials, with a transmission of 30.0%. In the same irradiation field, double plasterboard and double reinforced in thickness ceramic tile have similar transmission 30.0%. In addition the average transmitted X-ray energy and the dose area was reduce in 16 cm x 2 cm irradiation field compared to 7.5 cm x 7.5 cm irradiation field. In both irradiation fields, the glass block at first and then, the double reinforced in thickness ceramic tile and the double plasterboard provided lower transmission (%) and better radiation protection, from any other common building material for low energies.

Acknowledgements

I would like to express my most sincere gratitude to my Supervisor, Professor George Panayiotakis for giving me the opportunity to carry out this thesis under his supervision, providing me advises and support. I would like to thank him for the crucial support that he provided me throughout the time of preparing this thesis. It has been an honor to work with him throughout these years.

I would also like to express my very great appreciation to Professor Ioannis Kandarakis for their advice and co-operation during this research.

I would like to thank Assistant Professor Nektarios Kalyvas for giving me the inspiration to follow this path, helping me in every step of it. I would also like to thank him for continuous and substantial guidance at all stages of the doctoral dissertation.

My special thanks are extended to the staff of the Sismanoglio

General Hospital of Athens, for providing the X-ray Department and Department of Medical Physics to perform the necessary measurements. Especially I am truly indebted and thankful, Dr Xenophon Tsantilas for his extended and valuable advice and assistance throughout this project and work.

I would also like to especially thank for the support Dr Charalambos Delis for their advice and co-operation during this project.

Associate Professor George Fountos, whose expert advices and suggestions helped decisively work.

To my parents, Stefano and Argyro, for their valuable support, both morally and financially, throughout all these years of studies. Without their contribution it would not be possible to complete this thesis.

REFERENCES

1. Abbene L, La Manna A, Fauci F, Gerardi G, Stumbo S, Raso G. " X-ray spectroscopy and dosimetry with a portable CdTe device". Nuclear Instruments and Methods in Physics Research A 571 (2007).
2. Archer BR, "Recent history of the shielding of medical x-ray imaging facilities", Department of Radiology, Baylor College of Medicine, Houston, TX 77030, USA, Health Phys. 88(6):579-86 (2005).
3. Archer BR, Gray JE, "Important changes in medical x-ray imaging facility shielding design methodology. A brief summary of recommendations in NCRP Report No. 147", Baylor College of Medicine, Houston, Texas 77030, USA, Med Phys. Dec;32(12):3599-601 (2005).
4. Amptek, http://www.amptek.com/anczt1.html, (2015).
5. Akaagerger N M, Tyovenda A A, Ujah O F. "Evaluation of Quality Control Parameters of Half Value Layer, Beam Alignment and Collimator Test Tools on Diagnostic X-Ray Machines". International Journal of Science and Technology Volume 4 (2015).
6. Bell S. "A Beginner's Guide to Uncertainty of Measurement". National Physics Laboratory, UK (1999).
7. Bushberg J, Seibert A, Leidholdt E, Boone J. "The essential physics of medical imaging". 3th edition, Lippincott Williams & Wilkins, a Wolters Kluwer (2001).
8. Crowther J A. "The Biological Action of X Rays—A Theoretical Review". Br. J. Radiol. doi: http://dx.doi.org/10.1259/0007-1285-11-123-132 (1997).
9. Clarke R. International Commission on Radiation Protection, "21st century challenges in radiation protection and shielding: draft 2005 recommendations of ICRP". ICRP, Corner Cottage, Woolton Hill, Newbury, Berkshire, RG20 9XJ, Radiat Prot Dosimetry. 115(1-4):10-5 (2005).
10. DeWerd A L., Wagner K L."Characteristics of radiation detectors for diagnostic radiology". Applied Radiation and Isotopes 50 (1999).
11. Dos Santos M A, Conceicao M ., Mercia L O, Ricardo A L, Clovis A H." The use of CdTe detectors for dental X-ray spectrometry". Instrumentation Related To Nuclear Science And Technology. 978-85-99141 (2007).
12. Economides S, Hourdakis CJ, Kalivas N, Kalathatki M, Simantirakis G, Tritakis P, Manousaridis G, Vogiatzi S, Kipouros P, Boziari A, Kamenopoulou V. "Performance of medical radiographic X-ray systems in Greece for the time period 1998-2004". Physica Medica. 23, 107-114 (2007).
13. Edward R E., Herbert W. " Experimental Study of the Photon Energy Spectrum of Primary Diagnostic X-Rays ". Phys. Med. Biol. 225-238 (1966).
14. European Commission. "The safe use of radiographs in dental practice". Radiation Protection 136 (2004).
15. Fluke Biomedical model 451P-DE-SI, http://www.flukebiomedical.com/biomedical/usen/radiation-safety/survey meters/451p-pressurized-ion-chamber-radiation-detector-survey-meter.htm?PID=54793 (2015).
16. Greening J.R "Fundamentals of radiation dosimetry", Second Edition. Published by Taylor & Francis Group, Great Britain (1985).
17. Health Physics Society, Specialists in Radiation Safety. Instrumentation and measurements—Surveys and measurements (2014).
18. Herbert M., Parker. "Radiation Quantities and Units". Radiology. doi: http://dx.doi.org/10.1148/103.1.46 (1972).
19. IAEA Safety Reports Series No 39. "Applying radiation safety standards in diagnostic radiology and interventional procedures using X-rays". International Atomic Energy Agency (IAEA) (2006).
20. ICRP publication 103"The 2007 Recommendations of the International Commission on Radiological Protection".Ann ICRP.37(2-4):1-332 (2007).
21. International Atomic Energy Agency (IAEA). "Optimization of the radiological protection of patients undergoing radiography, fluoroscopy and computed tomography". IAEA Safety Standards Series (2004).
22. Jackson G, Brennan P, "Radio-protective aprons during radiological examinations of the thorax: an optimum strategy". UCD School of Diagnostic Imaging, Health Science Complex, University College Dublin, Oxford Journals, Mathematics & Physical Sciences & Medicine, Volume121, Issue4, 391-394 (2006).
23. Martini N, Koukkou V, Michail C, Sotiropoulou P, Kalyvas N, Kandarakis I, Nikiforidis G, Fountos G. "Pencil beam spectral measurements of Ce, Ho, Yb, and Ba powders for potential use in medical applications". Journal of Spectroscopy 563763 (2015).
24. McCullough E C., Cameron J R. "Exposure rates from diagnostic X-ray units". Br. J. Radiol. 43, 448–451 (1970).
25. Mc Vey G., Phil D., Weatherburn H. "A study of scatter in diagnostic x-ray rooms". Br. J. Radiol. 77, 28–38 (2004).
26. Le Galley P D. "A Type of GeigerMüller Counter Suitable for the Measurement of Diffracted Mo K Xrays". American Institute of Physics. doi: 10.1063/1.1752006 (1935).
27. Mellenberg D E, Sato Y, Thompson B H, Warnock N G. "Personnel exposure rates during simulated Biopsies with a real-time Ct Scanner". Acad. Radiol. 6, 687-690 (1999).
28. Michail C M, Spyropoulou V A, Fountos G P, Kalyvas N I, Valais I G., Kandarakis I, S. Panayiotakis G S. "Experimental and theoretical evaluation of a high resolution CMOS based detector under x-ray imaging conditions". IEEETNS. 58, 314–322 (2011).
29. Noto K., Koshida K.. "Estimation of 90° scattering coefficient in the shielding calculation of diagnostic X-ray equipment". Proceedings of the eleventh EGS4 users' meeting in Japan, KEK proceedings. 15, 107-113 (2003).
30. Noto K., Koshida K., Iida H, Yamamoto T, Kobayashi I, Kawabata C. "Investigation of scatter fractions for estimating leakage dose in medical X-ray imaging facilities". Radiol. Phys. Technol., 2, 138-144 (2009).
31. Odeh D, Ogbanje G, Jonah S.A. "X-Rays and Scattering from Filters Used in Diagnostic Radiology". International Journal of Scientific and Research Publications, Volume 3, Issue 7 (2013).
32. Ohba H, Fujibuchi T, Mita S, Horikoshi A, Iwanaga T, Ikebuchi H, Hosono M, "Research on the shielding evaluation method for medical X-ray imaging facilities", Hirosaki University Graduate School of Health Sciences, Japan, Nippon, Hoshasen, Gijutsu, Gakkai, Zasshi, 20;65(1):57-63 (2009).
33. PTW, http://www.ptw.de/diados_e_diagnostic_dosemeter.html, (2015).
34. Petrantonaki M., Kappas C., Efstathopoulos E., Theodorakos Y.,Panayiotakis G. "Calculating shielding requirements in diagnostic X-ray departments". Br. J. Radiol. 72 179-185 (1999)
35. Radiation Protection in Dentistry - Recommended Safety Procedures for the Use of Dental X-Ray Equipment - Safety code 30 Environmental Health Directorate Health Canada (1999).
36. Radiation Protection in Veterinary Medicine - Recommended Safety Procedures for Installation and Use of Veterinary X-Ray Equipment - Safety code 30 Environmental Health Directorate Health Canada (1991).
37. Radiopaedia, http://radiopaedia.org/ (2015).
38. Ramirez-Jime F J., Pez-Callejas R L., Benitez-Read J S.,Pacheco-Sotelo J O. "Considerations on the measurement of practical peak voltage in diagnostic radiology". Br. J. Radiol 76, 745–750 (2004).
39. Reddy D K S., Premachand K., Radha V., Murty K., Rama Rao J., Lakshminarayana V. "Photoelectric interaction below the K edge". Phys. Rev. A 13, 326 (1976).
40. Seibert J A. "X-Ray Imaging Physics for Nuclear Medicine Technologists. Part 1: Basic Principles of X-Ray Production". J Nucl Med Technol. 32:139–147 (2004).
41. Simpkin D J., and Dixon R. L. "Secondary shielding barriers for diagnostic X-rays facilities scatter and leakage revisited". Health Phys. 74, 350-365 (1998).
42. Sprawls P. "The Physical Principles of Medical Imaging, 2nd Ed" (1995), http://www.sprawls.org/ppmi2/
43. Tsalafoutas I A., Yakoumakis E., Sandilos P. "A model for calculating shielding requirements in diagnostic X-ray facilities". Br. J. Radiol 76, 731–737 (2003).
44. Tsalafoutas, I A. "Excessive leakage radiation measured on two mobile X-ray units due to the methodology used by the manufacturer to calculate and specify the required tube shielding". Br. J. Radiol. 79, 162–164 (2006).
45. Tucker D., Burnes G,. Wu X. "Molybdenum target x-ray spectra: A semiempirical method". Med. Phys. 18 (1991).
46. U.S Food and Drag Admistration, http://www.fda.gov/Radiation-EmittingProducts/RadiationEmittingProductsandProcedures/MedicalImaging/MedicalX-Rays/ucm115335.htm (2015).
47. Vlachos I, Tsantilas X, Kalyvas N, Delis H, Kandarakis I, Panayiotakis G. "Measuring scatter radiation in diagnostic X-rays for radiation protection purposes". Rad. Prot. Dosim. 165 382-385, doi:10.1093/rpd/ncv093 (2015).
48. Vlachos I, Tsantilas X, Fountos G, Delis H, Kandarakis I, Panayiotakis G. "Effect of common building materials in narrow shaped X-ray fields transmission". J. Phys.: Conf. Ser. 637 012034, doi:10.1088/1742-6596/637/1/012034 (2015).
49. Vanbeckevoort D, Ponette E, Baert AL, "The evolution of radioprotection", Department of Radiology, University Hospitals K.U., Leuven, Belgium, J Belge Radiol. 78(6):377-81 (1995).
50. Wrixon AD, "New ICRP recommendations", Castellezgasse 25/2/6, 1020 Vienna, Austria, J Radiol Prot. 2008 Jun;28(2):161-8. Epub May 22 (2008).
51. Zink E F. "X-ray tubes". RadioGraphics. doi: http://dx.doi.org/10.1148/radiographics.17.5.9308113 (1997).